International Journal of
Intelligent Systems and
Applications in Engineering
ISSN:2147-6799 www.atscience.org/IJISAE
Advanced Technology and Science
Original Research Paper

Comparison of Unsupervised Segmentation of Retinal Blood Vessels in Gray Level Image with PCA and Green Channel Image

Esra KAYA*[1], Ismail SARITAS[2], Murat CEYLAN[3]

Accepted : 24/09/2017 Published: 28/12/2017

Abstract: In this study, an unsupervised retina blood vessel segmentation process was performed on the gray level images with principal component analysis (PCA) and the green channel of the RGB image, which most clearly shows retinal vessels and the results were compared. The images were improved for a good segmentation by using contrast-limited adaptive histogram equalization (CLAHE), color intensity adjustment, morphological operations and median and Gaussian filtering. Retinal vessel structures were segmented with top-hat and bot-hat morphological operations and converted to binary image by using global thresholding. The average accuracy rate obtained for the gray level image with PCA after the study was 0.9443, while the average accuracy rate obtained for the green channel was 0.9685. The study was performed using 40 images in the DRIVE data set which is one of the most common retina data sets known.

Keywords: *Blood Vessel, Unsupervised Learning, Retina, Segmentation*

Introduction

Eye is one of the most important organs in the human body because of its vision and perception characteristics [1]. The eye may lose its functionality due to negative environmental factors or genetic problems. Functional disorders resulting from such problems can be understood from the structure of the eye or the blood vessels in the retina [1]. In addition, retinal blood vessels are also important because they can provide information about pathological diseases such as hypertension and diabetes [2]. For example, changes in the diameter of the vessel and development of neovascularization indicate diabetic retinopathy, while a decrease in the ratio of the diameter of the retinal arteries to the diameter of the vessels indicates hypertension. Another important feature of ocular blood vessels is that it is the only vein region in the human blood circulation system that can be examined from outside without requiring intervention [3]. Ophthalmologists diagnose patients by manually examining the status of blood vessels on retinal images obtained with high-resolution fundus cameras [2]. Although manual segmentation has high accuracy, it is a tedious, time-consuming operation that can be impossible in the presence of high-volume retinal data [3]. Thus, medical imaging has become a significant tool in recent times [4]. In general, fundus images have low contrast and background noise. Furthermore, the segmentation of blood vessels is difficult because the width, brightness and shape of blood vessels are variable. Thus, it is imperative to develop an effective image processing technique for an accurate automatic segmentation [3].

Different image processing techniques are used for retinal blood vessel segmentation. These are generally divided into segmentation with supervised and unsupervised learning. Unsupervised methods are rule-based and specify vein regions using the default rules for vessels. Unsupervised learning includes vein tracking, matched filtering, morphological processing, model-based algorithms and multi-scale analysis [3]. Supervised learning is more time-consuming and computationally expensive, as it requires training of complex classifiers that work with large data with different features [3].

If we give an example to unsupervised methods, a morphological component analysis (MCA) algorithm is used for retinal blood vessel segmentation by Imani et al. and it is aimed to prevent the formation of false positive vessel pixels in the area of diabetic lesions. As a result, the segmentation accuracy was 0,9524 for the DRIVE data set and 0,9590 for the STARE data set [5]. In another study conducted by Hassan et al., the images were enhanced with mathematical morphology and blood vessels were segmented by k-means clustering. As a result of experimental studies, 95.10% accuracy was obtained for the DRIVE data set [4]. Frucci et al. realized the segmentation process using the SEVERE method, which assigns retinal image pixels to 12 discrete directional information. The accuracy of 0.9550 and 0.9590 was obtained for the test and training images in the DRIVE data set, respectively [6]. Kovács et al. aimed to perform self-calibration of the retinal blood vessel segmentation system using template matching and contour reconstruction. Accuracy results were obtained for DRIVE and STARE data sets as 0,9494 and 0,9610, respectively [7]. In another unsupervised segmentation realized by Sing et al., a matched filter based on the function of Gumbel probability distribution was used and the accuracy rate was found 0,9522 for the DRIVE data set and 0,9270 for the STARE data set [2].

As an example of segmentation with supervised method, Soares et al. filtered the noise of the image by using 2-dimensional Gabor wavelet and thus, improved the vessel appearance. The accuracy rate obtained using Bayes classifier was 0,9614 [8]. In another study, Ceylan et al. achieved the accuracy of 98.56% by using complex wavelet transform and complex artificial neural network [9]. Vega et al. performed segmentation using a lattice neural network with dendritic processing and obtained 0,9412 accuracy for the DRIVE data set and 0,9483 accuracy for the STARE data set [10]. On the other hand, Wang et al. used convolutional neural network (CNN) for feature extraction and random forest (RF) classifier for segmentation to realize a hierarchical segmentation. As a result of the study, the accuracy of 0,9475 and 0,9751 were

[1-2] *Department of Electrical and Electronics Engineering, Faculty of Technology, Selcuk University, Konya – 42250, TURKEY*
[3] *Department of Electrical and Electronics Engineering, Faculty of Engineering, Selcuk University, Konya – 42250, TURKEY*
** Corresponding Author: Email: esrakaya@selcuk.edu.tr*

obtained for DRIVE and STARE data sets, respectively [11]. In another study performed by Ceylan et al., 98.44% accuracy for the DRIVE data set and 99.25% accuracy for the STARE data set were obtained using complex Ripplet-I transformation and complex valued artificial neural network [1].

In this study, an unsupervised segmentation method was applied on the gray level image obtained by principal component analysis (PCA) and green channel of RGB image and the results were compared.

1. Proposed Methodology

1.1. Image Acquisition

The system used consists of 40 original retinal images obtained from the DRIVE (Digital Retina Images for Vessel Extraction) data set, which is one of the most commonly used data sets, and the retinal images were acquired from a diabetic retinopathy screening program in The Netherlands by using a Canon CR5 non-mydriatic 3CCD camera with a 45 degree field of view (FOV) [12]. The database consists of 40 images which were divided into two categories: a training and a test set [12]. The segmentation for the training set was realized by a specialist ophthalmologist manually and the segmentation for the test set was realized by human observers, who were trained by an experienced ophthalmologist, manually by marking the pixels thought as vessel with 70% certainty [12].

1.2. Image Preprocessing and Segmentation

Green channel images are usually used as gray level images in studies realized on retinal images because the green channel of RGB images shows the difference between the blood vessels and the background best [13]. Converting the color image to gray level image with PCA also preserves the texture and color differences of the image [2]. There are several points to be taken into account and processes the image is subjected to during the conversion of the RGB image to grayscale using PCA, which are specified as follows;

- Firstly, the RGB image is converted to a uniform CIELa*b* color space which is based on human color perception[14]. The distance between any pair of image colors should be proportional to the distance between their gray values [15].
- The image is subjected to PCA which is a popular dimensionality reduction technique and its effectivity depends on the difference between luminance and chrominance channels [14]. If the ratio between the primary and the secondary axes is greater, it means more distinctive gray values are created for different colors [14].
- Finally, PCA requires an optimization technique to generate the grayscale image, which is a function of the chroma variation of the source image, by mixing the principal components [14, 16].

In this study, gray level images obtained from both PCA and green channel were used for comparison. Figure 1 shows the original image of the 19th test image in the data set. In Figure 2, both the gray level image with PCA and green channel image are shown.

The SNR value, which is the ratio of signal to noise for each gray image, is measured before contrast enhancement. This value gives information about the quality of gray level images [2]. The greater the SNR, the better the detail of the image is visible. The contrast parameters have been changed by taking into account the changes in the SNR value to achieve the best contrast value. SNR value is found by the ratio of the average of image pixel densities to the standard deviation of the pixel values [2]. After the calculation of SNR values of gray level images, contrast-limited adaptive histogram equalization (CLAHE) was used for contrast enhancement of images so that the recalculated SNR values were found to be higher, thus the details became more apparent.

Figure 1. 19_test.tif DRIVE image

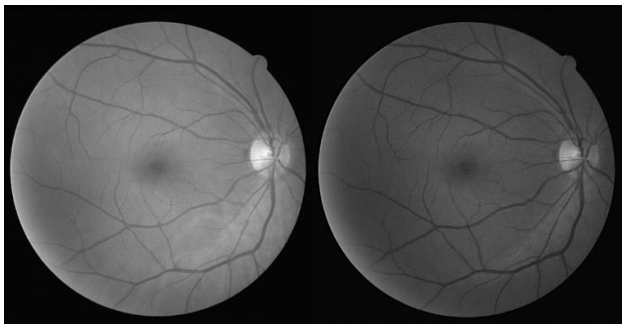

Figure 2. 19_test.tif Gray level with PCA and Green Channel Image

CLAHE method is different from normal histogram equalization because it works to optimize the local image contrast just like adaptive histogram equalization [17]. To achieve this, the image is split into tile like structures so that the contrast can be adjusted for all the regions separately [17]. The disadvantage of adaptive histogram equalization is the noise generation over the homogeneous regions such as the background of the image even though the respective region is more distinctive due to the contrast enhancement [17]. CLAHE method resolves this disadvantage by using a contrast limit known as clip limit for the regions [17]. This is realized by allowing only a maximum number of pixels belonging to the bins related to all local histograms and the pixels which are clipped are distributed uniformly over the whole histogram making it possible to preserve the former histogram count [17].

For this study, the distribution of CLAHE, meaning the desired histogram shape, was chosen as ‘rayleigh’ which is a bell shaped histogram and the contrast enhancement limit (clip limit) was chosen as 0.02 [18]. The best SNR value was obtained at this limit value. If the limit was changed to more or less than 0.02, the SNR value began to deteriorate. In Figure 3, the gray level and green channel images can be seen after they were improved with CLAHE.

After CLAHE, the density of the image pixels was changed and the color difference between the blood vessels and the background was increased. Salt-pepper noise was removed by applying median filtration on contrast enhanced images, and vascular structures were made more evident by applying Gaussian distributed matched filter [13]. The 2-dimensional Gaussian distribution is shown in the following form [13].

$$G(x,y) = \frac{1}{2\pi\sigma^2} exp(-\frac{x^2+y^2}{2\sigma^2}) \quad (1)$$

Additionally, top-hat morphological processing has been used to make vascular structures more prominent [13]. With the use of bottom-line morphological processing and subtraction of these two images from each other also resulted in blood vessels being separated from the background. After these processes, the images were converted to binary images by global thresholding and the complement of the images were taken. After complementing the images obtained by the specialists, the images were compared with each other and the correctly and incorrectly classified pixels were determined. The images obtained after the filtering process are shown in Figure 4, and the images obtained after the morphological processes are shown in Figure 5. In Figure 6, the complement of the binary images and the complement of the image obtained by specialists can be seen.

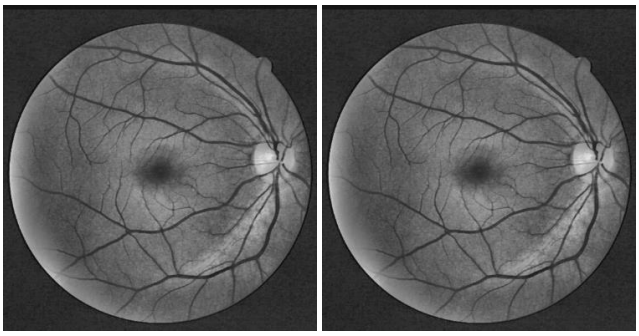

Figure 3. Gray Level and Green Channel Images After CLAHE

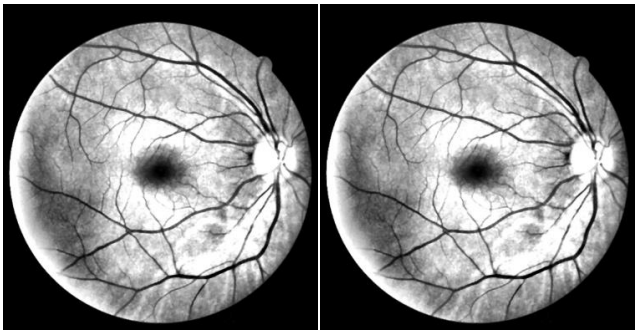

Figure 4. Gray Level and Green Channel Images After Filtering Process

Figure 5. Gray Level and Green Channel Images After Morpholoical Processes

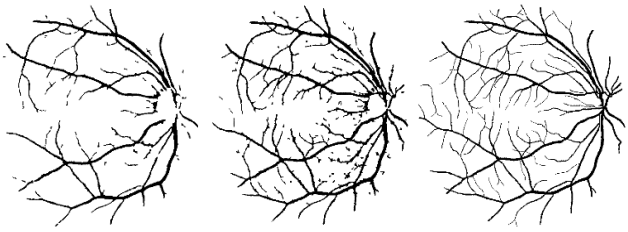

Figure 6. Segmented Gray level, Green Channel and Specialist Image

2. Results and Discussion

In the comparison of acquired images with specialist images, concepts such as true positive (TP), true negative (TN), false positive (FP) and false negative (FN) were used to evaluate the pixels. True positive refers to the classification of vessel pixels as vessels while true negative refers to the classification of background pixels as background. Also, false positive refers to the classification of background pixels as vessel and false negative refers to the classification of vessel pixels as background. The accuracy rate is given by the following formula.

$$Accuracy = (TP + TN)/(TP + TN + FP + FN) \quad (2)$$

According to the results obtained based on these values, the average accuracy rate of the segmentation for gray level image was found to be 0.9473, while the average accuracy of segmentation for green channel was 0.9685. In addition, the segmentation process took very short time which was a total of 17.9558 seconds for all 40 images. The results showed that segmentation in the green channel was more successful. In Table 1 and Table 2, the results of our study are given for comparison with other studies of unsupervised and supervised segmentation in the literature, respectively. Table 3 shows the SNR and accuracy results for all the images in the study and the best results obtained were indicated in a bold text format.

Table 1. Literature Studies of Unsupervised Segmentation

Author	*Year*	*Method*	*Accuracy*
İmani et al.	*2015*	*Morphological Component Analysis*	*0,9524*
Hassan et al.	*2015*	*Mathematical Morph. & k-means clustering*	*0,9510*
Frucci et al.	*2016*	*SEVERE*	*0,9570*
Kovács et al.	*2016*	*Template Matching & Contour Reconstruction*	*0,9494*
Singh et al.	*2016*	*Gumbel Probability Distributed Matched Filter*	*0,9522*
This study (Gray level with PCA)	*2017*	*CLAHE & Gaussian Matched Filter*	***0,9473***
This study (Green Channel)	*2017*	*CLAHE & Gaussian Matched Filter*	***0,9685***

Table 2. Literature Studies of Supervised Segmentation

Author	*Year*	*Method*	*Accuracy*
Soares et al.	*2006*	*2-D Gabor Wavelet & Bayes Classifier*	*0,9614*
Ceylan et al.	*2013*	*Complex Wavelet & Complex Valued ANN*	*0,9856*
Vega et al.	*2015*	*Lattice Neural Network with Dentritic Processing*	*0,9412*
Wang et al.	*2015*	*Convolutional Neural Network & Random Forest Classifier*	*0,9475*
Ceylan et al.	*2016*	*Complex Ripplet-I Transform & Complex Valued ANN*	*0,9844*
This study (Gray level with PCA)	*2017*	*CLAHE & Gaussian Matched Filter*	***0,9473***
This study (Green Channel)	*2017*	*CLAHE & Gaussian Matched Filter*	***0,9685***

Table 3. SNR and Accuracy Values Obtained For All Images

DRIVE Images	*SNR for Original Image*		*SNR for CLAHE Image*		*Accuracy*	
	Gray Level with PCA	*Green Channel*	*Gray Level with PCA*	*Green Channel*	*Gray Level with PCA*	*Green Channel*
01_test.tif	*1,8257*	*1,8421*	*2,5780*	*2,7433*	*0,9570*	*0,9720*
02_test.tif	*1,8542*	*1,8019*	*2,6166*	*2,6146*	*0,9347*	*0,9742*
03_test.tif	*1,9119*	*1,9187*	*2,5523*	*2,8421*	*0,9463*	*0,9720*
04_test.tif	*1,8252*	*1,7241*	*2,4498*	*2,5049*	*0,9492*	*0,9692*
05_test.tif	*1,8304*	*1,8054*	*2,5948*	*2,7608*	*0,9427*	*0,9706*
06_test.tif	*1,7308*	*1,6833*	*2,4269*	*2,5137*	*0,9449*	*0,9590*
07_test.tif	*1,7945*	*1,7813*	*2,4126*	*2,5495*	*0,9419*	*0,9689*
08_test.tif	*1,7355*	*1,5935*	*2,4763*	*2,5781*	*0,9356*	*0,9671*
09_test.tif	*1,7874*	*1,7548*	*2,5934*	*2,6718*	*0,9418*	*0,9591*
10_test.tif	*1,8854*	*1,8874*	*2,5695*	*2,8315*	*0,9546*	*0,9732*
11_test.tif	*1,7954*	*1,7450*	*2,5294*	*2,6104*	*0,9417*	*0,9688*
12_test.tif	*1,8195*	*1,7629*	*2,5537*	*2,6325*	*0,9471*	*0,9715*
13_test.tif	*1,8255*	*1,8339*	*2,5409*	*2,7274*	*0,9423*	*0,9588*
14_test.tif	*1,8398*	*1,7827*	*2,5924*	*2,6893*	*0,9527*	*0,9772*
15_test.tif	*1,9852*	*1,8468*	*2,6431*	*2,7032*	***0,9602***	***0,9820***
16_test.tif	*1,8043*	*1,7947*	*2,5438*	*2,6591*	*0,9475*	*0,9674*
17_test.tif	*1,7669*	*1,7138*	*2,3895*	*2,4457*	*0,9433*	*0,9614*
18_test.tif	*1,8237*	*1,7865*	*2,5451*	*2,5915*	*0,9508*	*0,9725*
19_test.tif	*1,7822*	*1,7579*	*2,4410*	*2,6056*	***0,9649***	***0,9797***
20_test.tif	*1,8251*	*1,8001*	*2,5961*	*2,7291*	*0,9588*	*0,9772*
21_training.tif	*1,7477*	*1,7044*	*2,4285*	*2,5566*	*0,9595*	*0,9749*
22_training.tif	*1,8047*	*1,7570*	*2,4178*	*2,5481*	*0,9380*	*0,9687*
23_training.tif	*1,7465*	*1,6578*	*2,3835*	*2,2626*	*0,9450*	*0,9744*
24_training.tif	*1,8059*	*1,7286*	*2,4780*	*2,4444*	*0,9165*	*0,9559*
25_training.tif	*1,8389*	*1,8110*	*2,6717*	*2,8400*	*0,9337*	*0,9573*
26_training.tif	*1,8780*	*1,8561*	*2,6325*	*2,7933*	*0,9523*	*0,9708*
27_training.tif	*1,7830*	*1,7153*	*2,4825*	*2,6058*	*0,9385*	*0,9667*
28_training.tif	*1,7961*	*1,8078*	*2,4695*	*2,5909*	*0,9460*	*0,9626*
29_training.tif	*1,8230*	*1,8338*	*2,4932*	*2,7433*	*0,9527*	*0,9752*
30_training.tif	*1,7921*	*1,6878*	*2,4292*	*2,5534*	*0,9535*	*0,9742*
31_training.tif	*1,7904*	*1,6788*	*2,3978*	*2,4488*	*0,9548*	*0,9690*
32_training.tif	*1,7852*	*1,7549*	*2,4618*	*2,5821*	*0,9484*	*0,9704*
33_training.tif	*1,8088*	*1,7621*	*2,4868*	*2,5483*	*0,9511*	*0,9687*
34_training.tif	*1,9171*	*1,8099*	*2,4299*	*2,3921*	*0,9232*	*0,9360*
35_training.tif	*1,9358*	*1,9072*	*2,6326*	*2,7518*	*0,9566*	*0,9787*
36_training.tif	*1,8234*	*1,8339*	*2,5453*	*2,6617*	*0,9423*	*0,9587*
37_training.tif	*1,8069*	*1,8137*	*2,4367*	*2,5177*	*0,9551*	*0,9678*
38_training.tif	*1,8091*	*1,8177*	*2,4785*	*2,6086*	*0,9514*	*0,9628*
39_training.tif	*1,7852*	*1,7578*	*2,5066*	*2,5743*	*0,9515*	*0,9700*
40_training.tif	*1,8367*	*1,8808*	*2,6034*	*2,8408*	*0,9624*	*0,9741*

3. Conclusion

Evaluation of the results showed that the segmentation process was successful and the green channel was more efficient for segmentation. In the future, different contrast enhancement, filtering, or morphological operations will be attempted to enhance the image and highlight the details for the purpose of improving unsupervised segmentation success.

References

[1] M. Ceylan and H. YAŞAR, "A novel approach for automatic blood vessel extraction in retinal images: complex ripplet-I transform and complex valued artificial neural network," *Turkish Journal of Electrical Engineering & Computer Sciences*, vol. 24, no. 4, pp. 3212-3227, 2016.

[2] N. P. Singh and R. Srivastava, "Retinal blood vessels segmentation by using Gumbel probability distribution function based matched filter," *Computer methods and programs in biomedicine*, vol. 129, pp. 40-50, 2016.

[3] S. Aslani and H. Sarnel, "A new supervised retinal vessel segmentation method based on robust hybrid features," *Biomedical Signal Processing and Control*, vol. 30, pp. 1-12, 2016.

[4] G. Hassan, N. El-Bendary, A. E. Hassanien, A. Fahmy, and V. Snasel, "Retinal blood vessel segmentation approach based on mathematical morphology," *Procedia Computer Science*, vol. 65, pp. 612-622, 2015.

[5] E. Imani, M. Javidi, and H.-R. Pourreza, "Improvement of retinal blood vessel detection using morphological component analysis," *Computer methods and programs in biomedicine*, vol. 118, no. 3, pp. 263-279, 2015.
[6] M. Frucci, D. Riccio, G. S. di Baja, and L. Serino, "Severe: Segmenting vessels in retina images," *Pattern Recognition Letters*, vol. 82, pp. 162-169, 2016.
[7] G. Kovács and A. Hajdu, "A self-calibrating approach for the segmentation of retinal vessels by template matching and contour reconstruction," *Medical image analysis*, vol. 29, pp. 24-46, 2016.
[8] J. V. Soares, J. J. Leandro, R. M. Cesar, H. F. Jelinek, and M. J. Cree, "Retinal vessel segmentation using the 2-D Gabor wavelet and supervised classification," *IEEE Transactions on medical Imaging*, vol. 25, no. 9, pp. 1214-1222, 2006.
[9] M. Ceylan and H. Yacar, "Blood vessel extraction from retinal images using complex wavelet transform and complex-valued artificial neural network," in *Telecommunications and Signal Processing (TSP), 2013 36th International Conference on*, 2013, pp. 822-825: IEEE.
[10] R. Vega, G. Sanchez-Ante, L. E. Falcon-Morales, H. Sossa, and E. Guevara, "Retinal vessel extraction using lattice neural networks with dendritic processing," *Computers in biology and medicine*, vol. 58, pp. 20-30, 2015.
[11] S. Wang, Y. Yin, G. Cao, B. Wei, Y. Zheng, and G. Yang, "Hierarchical retinal blood vessel segmentation based on feature and ensemble learning," *Neurocomputing*, vol. 149, pp. 708-717, 2015.
[12] J. Staal, M. D. Abramoff, M. Niemeijer, M. A. Viergever, and B. v. Ginneken, "Ridge-based vessel segmentation in color images of the retina," *IEEE Transactions on Medical Imaging*, vol. 23, no. 4, pp. 501-509, 2004.
[13] C. Zhu *et al.*, "Retinal vessel segmentation in colour fundus images using Extreme Learning Machine," *Computerized Medical Imaging and Graphics*, vol. 55, pp. 68-77, 2017.
[14] A. A. Gooch, S. C. Olsen, J. Tumblin, and B. Gooch, "Color2Gray: salience-preserving color removal," *ACM Trans. Graph.*, vol. 24, no. 3, pp. 634-639, 2005.
[15] K. Rasche, R. Geist, and J. Westall, "Re-coloring Images for Gamuts of Lower Dimension," in *Computer Graphics Forum*, 2005, vol. 24, no. 3, pp. 423-432: Wiley Online Library.
[16] G. R. Kuhn, M. M. Oliveira, and L. A. Fernandes, "An improved contrast enhancing approach for color-to-grayscale mappings," *The Visual Computer*, vol. 24, no. 7, pp. 505-514, 2008.
[17] K. Zuiderveld, "Contrast limited adaptive histogram equalization," in *Graphics gems IV*, S. H. Paul, Ed.: Academic Press Professional, Inc., 1994, pp. 474-485.
[18] Mathworks. (2017, 10.08.2017). *Contrast-Limited Adaptive Histogram Equalization*. Available: https://www.mathworks.com/help/images/ref/adapthisteq.html